Journal of Power and Energy Engineering, 2026, 14(4), 25-41
https://www.scirp.org/journal/jpee
ISSN Online: 2327-5901
ISSN Print: 2327-588X

Use of an Analytical Method for the Simulation of the Current-Voltage and Power-Voltage Characteristics of a Photovoltaic Solar Panel from the Manufacturer's Data

Arsène Eya'a Mvongbote, Hans Essone Obame, Honoré Gnanga

Laboratoire Pluridisciplinaire des Sciences (LAPLUS), Ecole Normale Supérieure de Libreville, Libreville, Gabon
Email: draeyaamvongbote@gmail.com

How to cite this paper: Mvongbote, A.E., Obame, H.E. and Gnanga, H. (2026) Use of an Analytical Method for the Simulation of the Current-Voltage and Power-Voltage Characteristics of a Photovoltaic Solar Panel from the Manufacturer's Data. *Journal of Power and Energy Engineering*, **14**, 25-41.
https://doi.org/10.4236/jpee.2026.144002

Received: January 22, 2026
Accepted: April 7, 2026
Published: April 10, 2026

Abstract

Global warming due to greenhouse gas emissions, mainly from fossil fuels, which reached an alarming level in 2022 [1], has led to a greater interest in renewable energy. Among these, solar energy occupies an important place because of its inexhaustible and non-polluting nature. Photovoltaic solar panels have become a preferred solution for the production of clean and sustainable electricity from solar energy, both for domestic and industrial applications. Renewable energies, including photovoltaics, are also very useful for electricity production in rural areas or hard-to-reach areas, especially in developing countries where electricity production is very low, whether domestic or industrial, is still very low. However, despite their potential, the performance of photovoltaic solar panels is strongly influenced by many factors, such as the climatic environment, irradiance, temperature, geographical position, humidity level, angle of incidence of the sun and heat losses [2] [3]. To improve their energy efficiency, it is essential to understand their electrical and thermal behavior. There are therefore several approaches to this subject, based on mathematical models, used in simulation software. Among the most widely used software is MATLAB, which is a computational and programming environment. The aim of this article is therefore to simulate the current-voltage and power-voltage characteristics from the data provided by the manufacturer of a polycrystalline photovoltaic solar panel model TSM-PD05.08 under several irradiations.

Keywords

Photovoltaic Solar Panel, Single-Diode Model, Analytical Model, Matlab Simulation, Manufacturer's Data

1. Introduction

In this paper, we will simulate the current-voltage and power-voltage characteristics of a TSM-PD05.08 polycrystalline photovoltaic solar panel model under multiple irradiations with Matlab 2019 from an analytical solution of the equation giving the expression of the model's photocurrent to a diode. The extraction of the model parameters will be carried out by making judicious and physically valid approximations in order to obtain simple analytical expressions to determine the model parameters with very good precision. In the first part, we present the structure of the solar cell and its working principle. In the second part we present the model of the photovoltaic cell used. In the third part, we present the methodology for extracting the parameters of the model used, and in the last part we present the equivalent diagram of the cell made with the Matlab 2019 software, which allows us to model the photovoltaic cell. The extracted values are also presented as well as the results of the simulations carried out on Matlab 2019, which we will compare to the experimental curves provided by the manufacturer. These results are presented, discussed and then commented on.

2. The Photovoltaic Cell [4]

It is an electronic component that converts solar energy into electrical energy, *i.e.* it converts the received photons into a direct electrical voltage. This is done through a process called the "photoelectric effect". This cell is usually made of semiconductor materials. The cells together form the photovoltaic solar module or panel. It can be designed on the basis of a homojunction or a heterojunction (**Figure 1**).

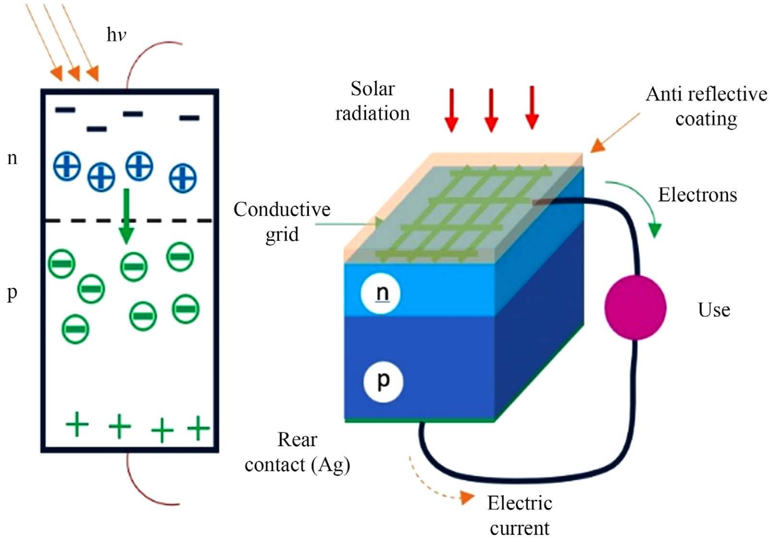

Figure 1. Illuminated n-p junction, photovoltaic cell.

2.1. Principle of Operation of a Solar Cell [4]

The photovoltaic cell absorbs photons from the incident light using the semiconductor material consisting of a conduction band and a valence band which, between them, is the band gap. If the energy of the incident photon is greater than the gap energy, then it transmits its energy to the electron which is in turn transported from the valence band to the conduction band, leaving a hole in the valence band. This absorption of the photon leads to the creation of electron-hole pairs. If the energy of the photon is insufficient, then it is not absorbed and it passes through the material without transmitting its energy. After creating electron-hole pairs, if the carriers are not extracted quickly enough on either side of the cell, then there will be a recombination between the electron and the hole. To do this, an internal electric field is imposed on the cell to separate the carriers and to orient positively and negatively charged carriers in the opposite direction. The creation of the internal electric field is due to the use of a P-N junction consisting of two semiconductor materials doped respectively, positively and negatively. When the two semiconductors come into contact, three regions appear: N-doped region, P-doped region, and an interface between the other two. In the latter, there is diffusion of free carriers, majority and recombination with each other. This area is called the depletion zone (ZCE space load zone). The charges carried by doped atoms that are no longer in the vicinity of a carrier free of opposite charges are responsible for the formation of an electric field. The latter is the basis for the separation of electron-photo hole pairs generated, of course under illumination, and for the attraction of électrons in the N-doped material and the holes in the P-doped material, all this gives rise to a photo-current. In summary, the photovoltaic conversion in a solar cell is based on:

- Light absorption and generation of electron-hole pairs.
- The scattering and separation of electron-hole pairs are created by photons.
- Charge collection: the electro-hole pairs are returned by means of an electric field from the junction to the regions where they will be in the majority (**Figure 2**). That is to say the electrons towards the emitter (N-type region) and the holes towards the base (P-type region).

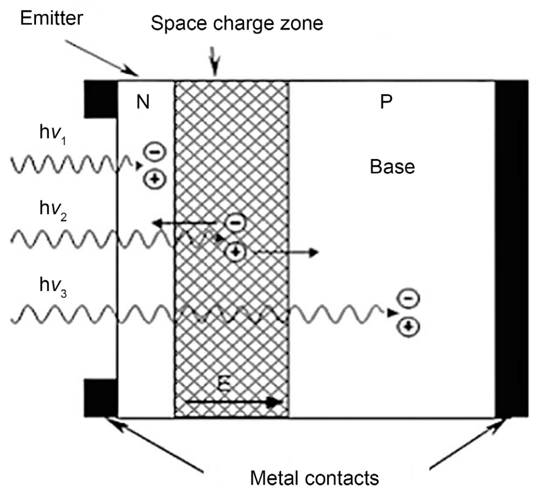

Figure 2. Operating principle of a photovoltaic cell.

2.2. Modeling the Solar Cell [5]

2.2.1. Ideal Model

To maximize the power output extracted from a PV power plant with the help of MPPT control, understanding and modeling of PV cells is required. The ideal equivalent circuit of a solar cell is a current source in parallel with a single diode. The equivalent diagram of the ideal simulated solar cell with a single diode is shown in **Figure 3**.

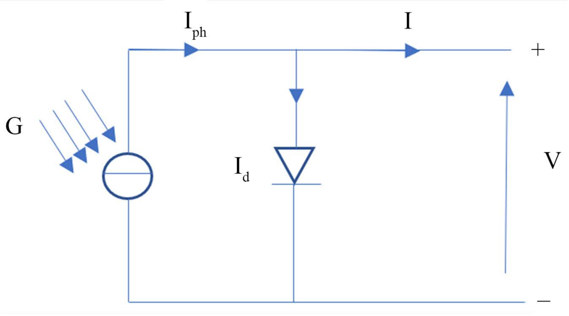

Figure 3. Equivalent diagram of the ideal solar cell.

In **Figure 3**, G is the irradiance due to sunlight, I_{ph} is the photo-current generated, I_d is the diode current, I is the output current, and V is the terminal voltage. The I-V characteristic of the ideal solar cell with single diode is given by:

$$I = I_{Ph} - I_0\left(e^{\frac{qV}{aKT}} - 1\right) \tag{1}$$

2.2.2. Model with Series Resistor

Greater accuracy can be introduced into the model by adding a R_s series resistor. The configuration of the simulated solar cell with a single diode and a series resistor is shown in **Figure 4**.

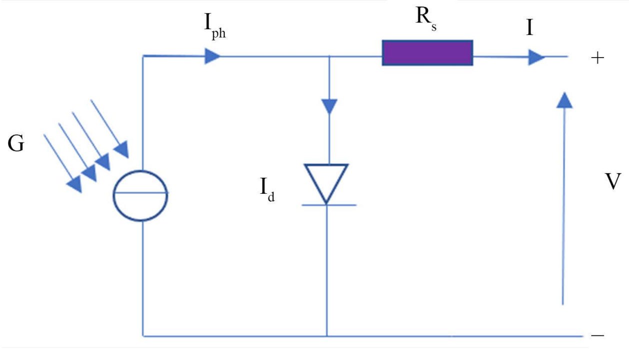

Figure 4. Equivalent diagram of the solar cell with series resistor.

The I-V characteristic is given by:

$$I = I_{Ph} - I_0\left(e^{\frac{q(V+R_sI)}{aKT}} - 1\right) \tag{2}$$

2.2.3. Model with Series Resistor and Shunt

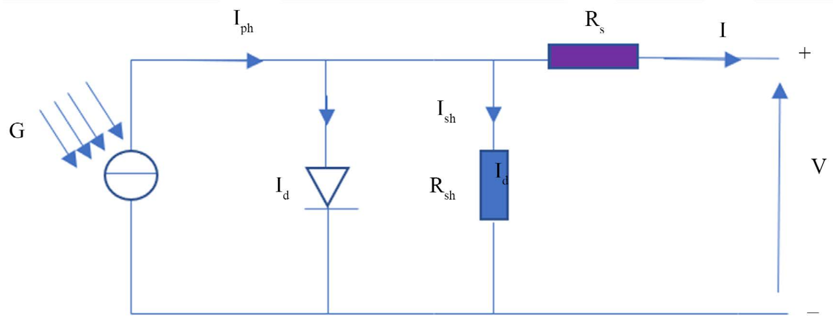

Figure 5. Equivalent diagram of the solar cell with series resistor and shunt.

The current-voltage characteristic of the single diode solar cell, with series and shunt resistors is given by:

$$I_{pv}=I_{Ph}-I_0\left(\mathrm{e}^{\frac{q(V+R_S I)}{aKT}}-1\right)-\left(\frac{q\left(V+R_s I\right)}{R_{sh}}\right) \tag{3}$$

3. Methodology for Extracting Model Parameters

For our study, we have chosen the one-diode model taking into account all the effects whose equivalent electrical pattern is presented in Figure 5. This model is composed of a photogenerator in parallel with a diode, as a generator is not perfect and to take into account dissipative effects, two resistors have been introduced, the R_S series resistor and the parallel resistor or R_{sh} shunt [6] [7]. The series resistance is due to the contribution of the base resistors, the front of the junction as well as the front and rear contacts. The shunt resistance is due to a leakage current at the junction [8]. The solar panel studied here has cells in series, so we will use the following relation N_S [9].

$$I=I_{Ph}-I_0\left(\mathrm{e}^{\frac{q(V+R_S I)}{aN_S KT}}-1\right)-\left(\frac{q\left(V+R_s I\right)}{R_{sh}}\right) \tag{4}$$

With

$$I_{Ph}=I_0+K_i\left(T-T_r\right)\frac{G}{G_r} \tag{5}$$

And,

$$I_0=I_{rr}\left[\frac{T}{T_r}\right]^3\mathrm{e}^{\frac{qE_G}{Ka}\left(\frac{1}{T_r}-\frac{1}{T}\right)} \tag{6}$$

By laying $V_T=\dfrac{aN_S kT}{q}$. The equation becomes:

$$I=I_{Ph}-I_0\left(\mathrm{e}^{\frac{q(V+R_S I)}{V_T}}-1\right)-\left(\frac{q\left(V+R_s I\right)}{R_{sh}}\right) \tag{7}$$

The model parameters are summarized in Table 1.

Table 1. Parameters of the single-diode model.

I_{ph}	Photo-courant
I_0	Courant de saturation
q	La charge élémentaire
R_s	Résistance série
R_{sh}	Résistance shunt
N_s	Nombre de cellules en série
N_p	Nombre de cellules en parallèle
K	Constante de Boltzmann
T	Température Ambiante
a	Coefficient d'idéalité
I_{rr}	Courant d'irradiation de reférence
K_i	Le coefficient de température du courant de court-circuit.
T_r	Température de référence
G	Ensoleillement reçu par le panneau
G_r	Ensoleillement référentiel
E_G	Gap energy of silicon
T_r	Température ambiante de référence

In the following, we present the methodology for extracting the model parameters from the equations of the model, which has a diode with series resistance and shunt. It is therefore a question of determining the R_S series resistor, the shunt resistor R_{sh}, the saturation current I_0, the ideality coefficient a and the photo-current I_{ph}.

3.1. Determination of Courant I_{ph}

We will start from Equation (4) under short-circuit conditions: $V = 0$ and $I = I_{sc}$ A normal value of the diode voltage is very low, the saturation current is of the order of a few nanoamperes $R_s V_d \approx R_s I_{sc}$, With all these approximations, the following two terms tend to zero:

$$I_0\left(e^{\frac{qR_S I_{pv}}{aN_S KT}}-1\right)\approx 0 \tag{8}$$

$$\frac{R_s I_{pv}}{R_{sh}}\approx 0 \tag{9}$$

We finally have:

$$I_{ph}\approx I_{sc} \tag{10}$$

3.2. Determination of Shunt Resistance

For different values of the slope of the curve, the current-voltage characteristic is not the same by deriving Equation (4) we obtain:

$$\frac{\mathrm{d}I}{\mathrm{d}V}=-\frac{I_0}{V_T}\left(\mathrm{e}^{\frac{(V+R_S I)}{V_T}}\left(1+R_S\frac{\mathrm{d}I}{\mathrm{d}V}\right)\right)-\frac{1}{R_{sh}}-\frac{R_S}{R_{sh}}\frac{\mathrm{d}I}{\mathrm{d}V} \tag{11}$$

$$\frac{\mathrm{d}I}{\mathrm{d}V}\left(1+\frac{R_S}{R_{sh}}+\frac{I_0R_S}{V_T}\mathrm{e}^{\frac{(V+R_S I)}{V_T}}\right)=-\frac{I_0}{V_T}\mathrm{e}^{\frac{(V+R_S I)}{V_T}}-\frac{1}{R_{sh}} \tag{12}$$

The following two terms tend to zero:

$$\frac{R_S}{R_{sh}}\approx 0 \tag{13}$$

Car $R_{sh}\gg R_s$, in short-circuit conditions, and knowing that the saturation current is of the order of a few nano amperes:

$$\frac{I_0R_S}{V_T}\mathrm{e}^{\frac{(V+R_S I)}{V_T}}=\frac{I_0R_S}{V_T}\mathrm{e}^{\frac{R_S I_{sc}}{V_T}}\approx 0 \tag{14}$$

We finally obtain:

$$R_{sh}=-\frac{\mathrm{d}V}{\mathrm{d}I}\quad\text{in short-circuit} \tag{15}$$

It is therefore the opposite of the inverse of the slope of the current-voltage characteristic in short-circuit.

3.3. Determination of the R_S Series Resistor

To determine the series resistance, we must place ourselves in the open circuit conditions, $I=0$ and $V=V_{OC}$ Equation (4) becomes:

$$0=I_{ph}-I_0\left(\mathrm{e}^{\frac{V_{OC}}{V_T}}-1\right)-\frac{V_{OC}}{R_{sh}} \tag{16}$$

or $I_{ph}\approx I_{sc}$

$$0=I_{sc}-I_0\left(\mathrm{e}^{\frac{V_{OC}}{V_T}}-1\right)-\frac{V_{OC}}{R_{sh}} \tag{17}$$

With $R_{sh}\gg R_s$. We finally have:

$$I_{sc}\approx I_0\left(\mathrm{e}^{\frac{R_S I_{SC}}{V_T}}-1\right) \tag{18}$$

Equation (11) becomes:

$$\frac{\mathrm{d}I}{\mathrm{d}V}\left(1+R_S\left(\frac{1}{R_{sh}}+\frac{I_{sc}}{V_T}\right)\right)=-\frac{I_{SC}}{V_T}-\frac{1}{R_{sh}} \tag{19}$$

And,

$\frac{1}{R_{sh}}\ll 0$, we finally

$$R_S=-\frac{\mathrm{d}V}{\mathrm{d}I}_{oc}-\frac{V_T}{I_{sc}} \tag{20}$$

in open circuit conditions.

3.4. Determination of I_0 Saturation Current

Considering Equation (4) under open circuit conditions, the equation becomes: $V = V_{OC}$ and $I = 0$

$$I_0\left(\mathrm{e}^{\frac{V+IR_S}{V_T}} - 1\right) = I_0 \mathrm{e}^{\frac{V_{oc}}{V_T}} = I_{SC} - \frac{V_{OC}}{R_{Sh}} \tag{21}$$

By dividing equality by $\mathrm{e}^{\frac{V_{oc}}{V_T}}$. We find:

$$I_0 = \frac{I_{sc} - \frac{V_{oc}}{R_{sh}}}{\mathrm{e}^{\frac{V_{oc}}{V_T}}} \tag{22}$$

3.5. Determination of the Coefficient of Ideality *a*

This factor is determined from the maximum operating point, $V = V_{mp}$ and $I = I_{mp}$ with $I_{ph} \approx I_{sc}$ We then have:

$$I_{mp} = I_{sc} - I_0\left(\mathrm{e}^{\frac{V_{mp}+R_S I_{mp}}{V_T}} - 1\right) - \left(\frac{V_{mp} + R_S I_{mp}}{R_{Sh}}\right) \tag{23}$$

To determine the model parameters, after determining the shunt resistance, we need to solve the following system of three nonlinear equations:

$$\begin{cases} R_S = -\dfrac{\mathrm{d}V}{\mathrm{d}I} - \dfrac{V_T}{I_{sc}} \\ I_0 = \dfrac{I_{sc} - \frac{V_{oc}}{R_{sh}}}{\mathrm{e}^{\frac{V_{oc}}{V_T}}} \\ I_{mp} = I_{sc} - I_0\left(\mathrm{e}^{\left(\frac{V_{mp}+R_S I_{mp}}{V_T}\right)} - 1\right) - \left(\dfrac{V_{mp} + R_S I_{mp}}{R_{Sh}}\right) \end{cases} \tag{24}$$

To solve this nonlinear system, numerical methods such as Newton-Raphson are best suited, but here we will propose an analytical solution to this system of equations by making some approximations. The following terms tend to zero because $R_{sh} \gg R_s$.

$$\frac{V_{mp} + R_S I_{mp}}{R_{Sh}} \approx 0 \tag{25}$$

$$\frac{V_{oc}}{R_{sh}} \approx 0 \tag{26}$$

The system of equations then becomes:

$$\begin{cases} R_S = \frac{\mathrm{d}I}{\mathrm{d}V}_{oc} - \frac{V_T}{I_{sc}} \\ I_0 = I_{sc}\mathrm{e}^{-\frac{V_{oc}}{V_T}} \\ I_{mp} = I_{sc} - I_0\left(\mathrm{e}^{\left(\frac{V_{mp}+R_S I_{mp}}{V_T}\right)} - 1\right) \end{cases} \tag{27}$$

We also:

$$V_{mp} \gg R_S I_{mp} \text{ and } \mathrm{e}^{\frac{V_{mp}}{V_T}} \gg 1 \tag{28}$$

We will finally have the following system:

$$\begin{cases} R_S = -\frac{\mathrm{d}V}{\mathrm{d}I}_{oc} - \frac{V_T}{I_{sc}} \\ I_0 = I_{sc}\mathrm{e}^{-\frac{V_{oc}}{V_T}} \\ I_{mp} = I_{sc} - I_0\mathrm{e}^{\left(\frac{V_{mp}+R_S I_{mp}}{V_T}\right)} \end{cases} \tag{29}$$

By laying $c = \frac{\mathrm{d}V}{\mathrm{d}I}_{oc}$ on *a*:

$$\begin{cases} R_S = -c - \frac{V_T}{I_{sc}} \\ I_0 = I_{sc}\mathrm{e}^{-\frac{V_{oc}}{V_T}} \\ I_{mp} = I_{sc} - I_{sc}\mathrm{e}^{\left(\frac{V_{mp}+R_S I_{mp}-V_{oc}}{V_T}\right)} \end{cases} \tag{30}$$

$$\begin{cases} R_S = -c - \frac{V_T}{I_{sc}} \\ I_0 = I_{sc}\mathrm{e}^{-\frac{V_{oc}}{V_T}} \\ I_{mp} = I_{sc}\left[1 - \mathrm{e}^{\left(\frac{V_{mp}+R_S I_{mp}-V_{oc}}{V_T}\right)}\right] \end{cases} \tag{31}$$

$$\begin{cases} R_S = -c - \frac{V_T}{I_{sc}} \\ I_0 = I_{sc}\mathrm{e}^{-\frac{V_{oc}}{V_T}} \\ \frac{I_{mp}}{I_{sc}} = 1 - \mathrm{e}^{\left(\frac{V_{mp}+R_S I_{mp}-V_{oc}}{V_T}\right)} \end{cases} \tag{32}$$

$$\begin{cases} R_S = -c - \frac{V_T}{I_{sc}} \\ I_0 = I_{sc}\mathrm{e}^{-\frac{V_{oc}}{V_T}} \\ \mathrm{e}^{\left(\frac{V_{mp}+R_S I_{mp}-V_{oc}}{V_T}\right)} = 1 - \frac{I_{mp}}{I_{sc}} \end{cases} \tag{33}$$

$$\begin{cases} R_S = -c - \dfrac{V_T}{I_{sc}} \\ I_0 = I_{sc}\mathrm{e}^{-\frac{V_{oc}}{V_T}} \\ \dfrac{V_{mp} + R_S I_{mp} - V_{oc}}{V_T} = \ln\left(1 - \dfrac{I_{mp}}{I_{sc}}\right) \end{cases} \tag{34}$$

$$\begin{cases} R_S = -c - \dfrac{V_T}{I_{sc}} \\ I_0 = I_{sc}\mathrm{e}^{-\frac{V_{oc}}{V_T}} \\ \dfrac{R_S I_{mp}}{V_T} = \left(\dfrac{V_{oc} - V_{mp}}{V_T}\right) + \ln\left(1 - \dfrac{I_{mp}}{I_{sc}}\right) \end{cases} \tag{35}$$

$$\begin{cases} R_S = -c - \dfrac{V_T}{I_{sc}} \\ I_0 = I_{sc}\mathrm{e}^{-\frac{V_{oc}}{V_T}} \\ R_s = \dfrac{V_T}{I_{mp}}\left[\left(\dfrac{V_{oc} - V_{mp}}{V_T}\right) + \ln\left(1 - \dfrac{I_{mp}}{I_{sc}}\right)\right] \end{cases} \tag{36}$$

$$-c - \frac{V_T}{I_{sc}} = \left(\frac{V_{oc} - V_{mp}}{I_{mp}}\right) + \frac{V_T}{I_{mp}}\ln\left(1 - \frac{I_{mp}}{I_{sc}}\right) \tag{37}$$

$$\frac{V_T}{I_{mp}}\ln\left(1 - \frac{I_{mp}}{I_{sc}}\right) + \frac{V_T}{I_{sc}} = -c - \left(\frac{V_{oc} - V_{mp}}{I_{mp}}\right) \tag{38}$$

$$V_T \ln\left(1 - \frac{I_{mp}}{I_{sc}}\right) + \frac{V_T}{I_{sc}} = -c - \left(\frac{V_{oc} - V_{mp}}{I_{mp}}\right) \tag{39}$$

$$V_T\left[\ln\left(1 - \frac{I_{mp}}{I_{sc}}\right) + \frac{1}{I_{sc}}\right] = -c - \left(\frac{V_{oc} - V_{mp}}{I_{mp}}\right) \tag{40}$$

$$V_T = -\frac{\left[c + \left(\dfrac{V_{oc} - V_{mp}}{I_{mp}}\right)\right]}{\left[\ln\left(1 - \dfrac{I_{mp}}{I_{sc}}\right) + \dfrac{1}{I_{sc}}\right]} \tag{41}$$

$$\frac{aN_S kT}{q} = -\frac{\left[c + \left(\dfrac{V_{oc} - V_{mp}}{I_{mp}}\right)\right]}{\left[\ln\left(1 - \dfrac{I_{mp}}{I_{sc}}\right) + \dfrac{1}{I_{sc}}\right]} \tag{42}$$

$$a = -\frac{q}{N_S kT}\frac{\left[c + \left(\dfrac{V_{oc} - V_{mp}}{I_{mp}}\right)\right]}{\left[\ln\left(1 - \dfrac{I_{mp}}{I_{sc}}\right) + \dfrac{1}{I_{sc}}\right]} \tag{43}$$

4. Results and Discussions

The parameters of the photovoltaic panel studied provided by the manufacturer and the parameters extracted from the model are presented in Table 2.

Table 2. Electric paddle gauges provided by the manufacturer.

ELECTRICAL DATA (STC)				
Peak Power Watts-$PMAX$ (Wp)*	255	260	265	270
Power Output Tolerance-$PMAX$ (W)	0 - +5			
Maximum Power Voltage- $VMPP$ (V)	30.5	30.6	30.8	30.9
Maximum Power Current-$IMPP$ (A)	8.37	8.50	8.61	8.73
Open Circuit Voltage- VOC (V)	38.1	38.2	38.3	38.4
Short Circuit Current-ISC (A)	8.88	9.00	9.10	9.18
Module Efficiency ηm (%)	15.6	15.9	16.2	16.5

STC: Irradiance 1000 W/m^2, Cell temperature 25˚C, Air Masse AMI.5.1; *test Tolerance: 3%.

ELECTRICAL DATA (NOCT)				
Maximum Power-$PMAX$ (Wp)	189	193	197	200
Maximum Power Voltage- $VMPP$ (V)	28.2	28.4	28.6	28.7
Maximum Power Current-$IMPP$ (A)	6.71	6.81	6.89	6.97
Open Circuit Voltage- VOC (V)	35.3	35.4	35.5	35.5
Short Circuit Current-ISC (A)	7.17	7.27	7.35	7.41

NOCT: Irradiance at 800 W/m^2, Ambient Temperature 20˚C; Wind Speed 1 m/s.

MECHANICAL DATA	
Solar Cells	Multicrystalline 156 × 156 mm (6 inches)
Cell ientation	60 cells (6 × 10)
Module Dimensions	1650 × 992 × 35 mm (65.0 × 39.1 × 1.38 inches)
Weight	18.6 kg (41.0 lb)
Glass	3.2 mm (0.13 inches), High Transmission, AR Coated Tempered Glass
Backsheet	White (PD05.08); Black (PD05.05)
Frame	Black (PD05.08, PD05.05)
J-Box	IP 67 or IP 68 rated
Cables	Photovoltaic Technology Cable 4.0 mm^2 (0.006 inches^2), 1000 mm (39.4 inches)
Connector	MC4 Compatible or Amphenol H4/UTX
Fire Type	Type 1 or Type 2

TEMPERATURE RATINGS	
Nominal Operating Cell Temperature (NOCT)	44˚C (±2˚C)
Temperature Coefficient of $PMAX$	−0.41%/˚C
Temperature Coefficient of VOC	−0.32%/˚C
Temperature Coefficient of ISC	0.05%/˚C

Table 3 below shows the panel parameters recorded on the curves reconstructed from the current-voltage and power-voltage curves provided by the manufacturer, as well as the model parameters extracted from the extraction methodology presented in the theoretical part.

Table 3. Extracts model settings.

Irradiation (W/m²)	200	400	600	800	1000
V_{mp} (A)	27.1154	28.4615	28.4615	30	30.6020
I_{mp} (A)	1.6967	3.3504	5.1151	6.5729	8.7939
I_{sc} (A)	1.7481	3.5038	5.2685	7.0588	9.2007
V_{oc} (V)	34.7115	35.7692	36.3462	36.8269	38.3930
R_{sh} (Ω)	6.3888 10^{15}	inf	1.9422 10^{15}	inf	inf
R_s (Ω)	0.0324	0.0189	0.0126	0.0102	6.035610^{-3}
a	0.7040	0.5986	0.6277	0.4947	0.9288
I_0 (A)	3.4070 10^{-10}	3.4555 10^{-10}	3.5830 10^{-10}	3.5222 10^{-10}	1.6742 10^{-10}
I_{ph} (A)	1.7481	3.5038	5.2685	7.0588	9.2007

The values extracted from the ideality coefficient a are not physically valid, for the simulation we have taken a = 1 because the value of the ideality factor is between 1 and 2 for silicon junctions. For the simulation in Matlab 2019, we entered the values of the extracted parameters, first creating the electrical circuit we want to simulate. We therefore made the following electrical circuit under Matlab 2019, consisting of a solar cell irradiated by a light source E, a variable resistor, an ammeter in series A to measure the current of the cell, a voltmeter V in parallel to measure the voltage of the cell. We then realize the product of the voltage by the current to obtain the power, then we display the I-V and P-V curves. To run the simulation in Matlab, we chose the single-diode model by clicking on the photo generator and entering the extracted parameters (**Figure 6**).

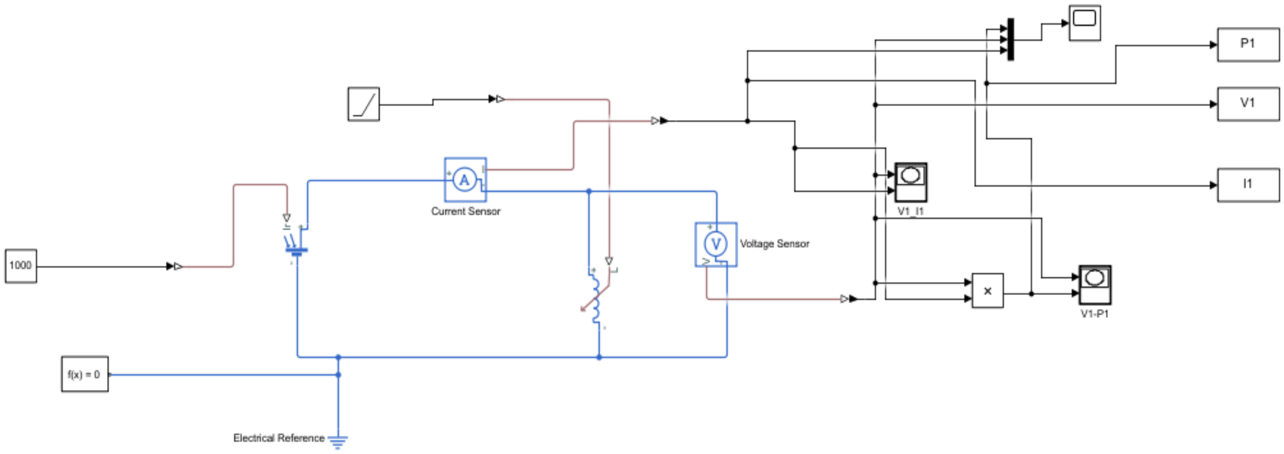

Figure 6. Electrical diagram equivalent to a photovoltaic cell made under Matlab 2019.

The results of the simulations obtained are presented on the curves below. The simulated values are compared with the measured values. Figures 7-16 below represent the results of the continuous line simulations compared to the values provided by the manufacturer in dashed lines, these values provided by the manufacturer were obtained from the data sheet provided by the manufacturer via the Plotdigitizer online software which allowed us to reconstruct the characteristics provided point by point for the radiation ranging from 200 W/m² to 1000 W/m².

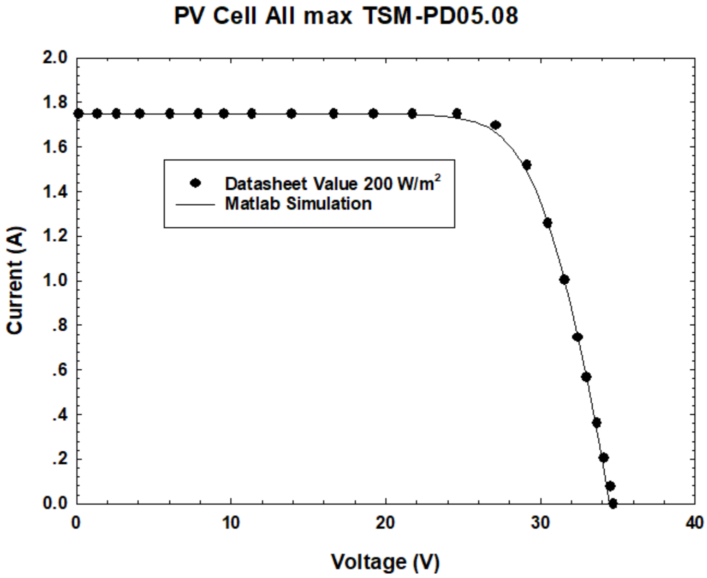

Figure 7. Comparison of the Matlab simulation with the manufacturer's values of the current-voltage characteristic for irradiation of 200 W/m².

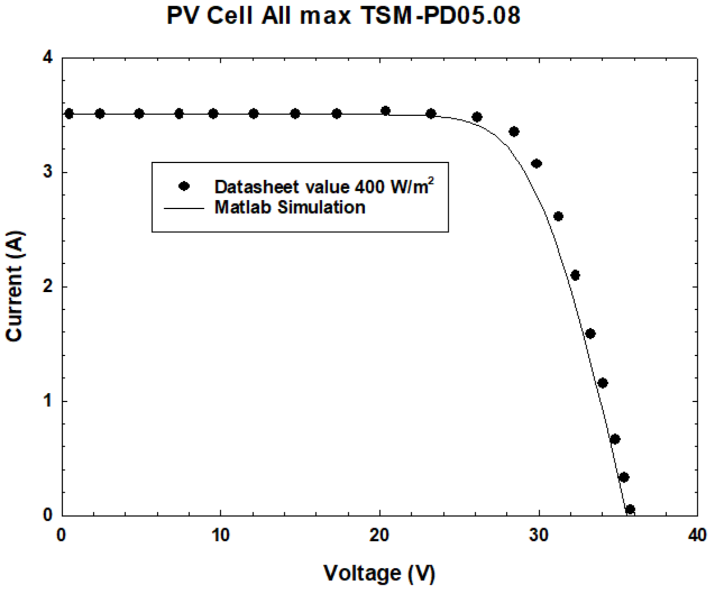

Figure 8. Comparison between the Matlab simulation and the values provided by the manufacturer of the current-voltage characteristic for an irradiation of 400 W/m².

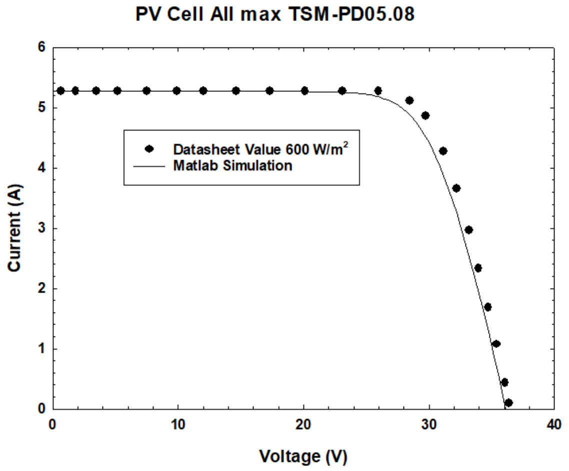

Figure 9. Comparison between the Matlab simulation and the values provided by the manufacturer of the current-voltage characteristic for an irradiation of 600 W/m^2.

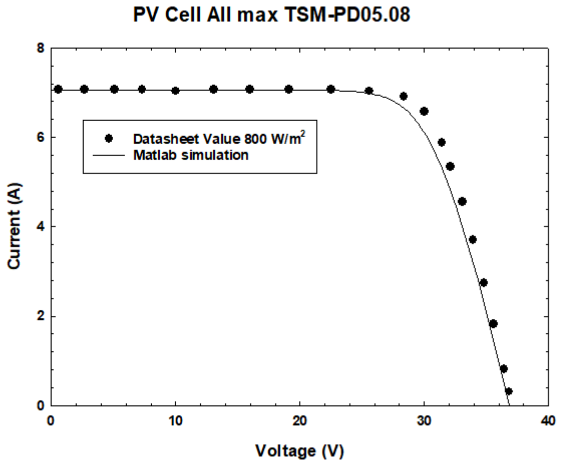

Figure 10. Comparison between the Matlab simulation and the values provided by the manufacturer of the current-voltage characteristic for an irradiation of 800 W/m^2.

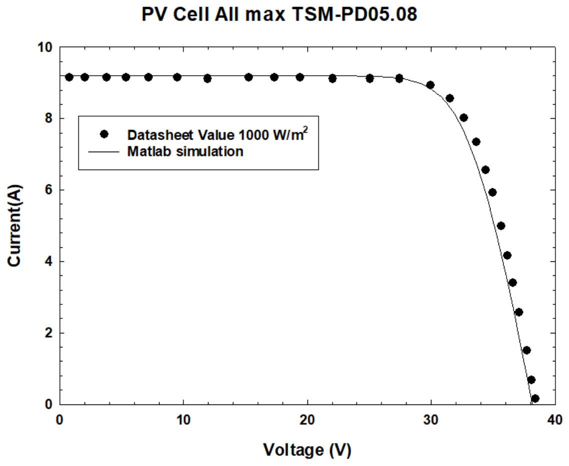

Figure 11. Comparison between the Matlab simulation and the values provided by the manufacturer of the current-voltage characteristic for an irradiation of 1000 W/m^2.

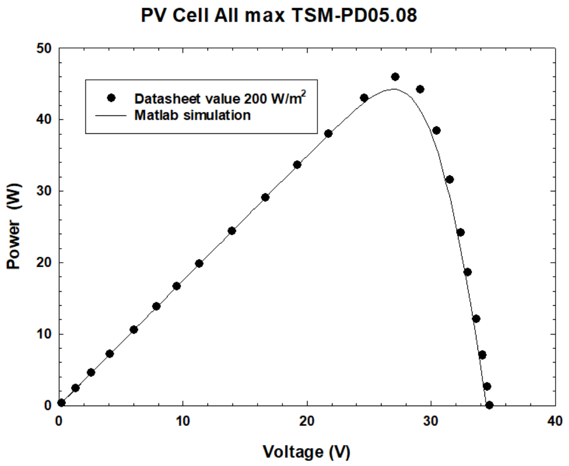

Figure 12. Comparison between the Matlab simulation and the values provided by the manufacturer of the power-voltage characteristic for an irradiation of 200 W/m^2.

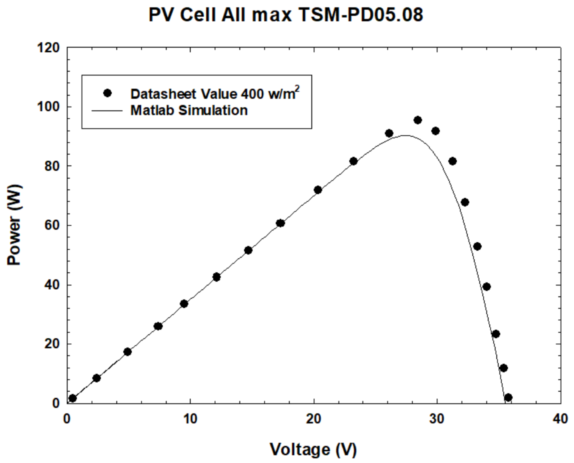

Figure 13. Comparison between the Matlab simulation and the values provided by the manufacturer of the power-voltage characteristic for an irradiation of 400 W/m^2.

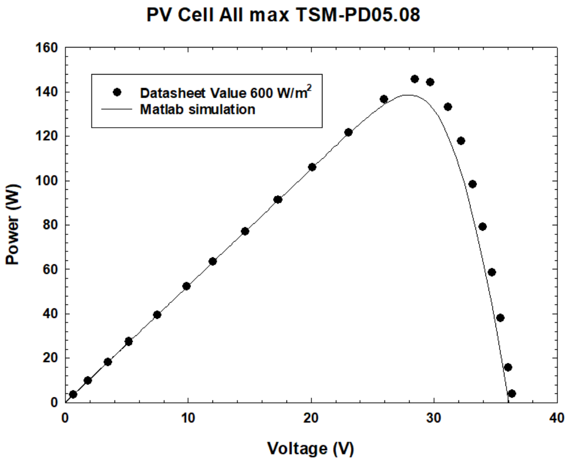

Figure 14. Comparison between the Matlab simulation and the values provided by the manufacturer of the power-voltage characteristic for an irradiation of 600 W/m^2.

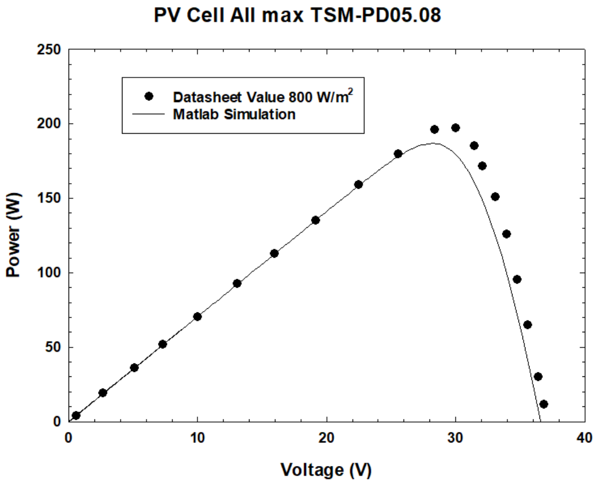

Figure15. Comparison between the Matlab simulation and the values provided by the manufacturer of the power-voltage characteristic for an irradiation of 800 W/m^2.

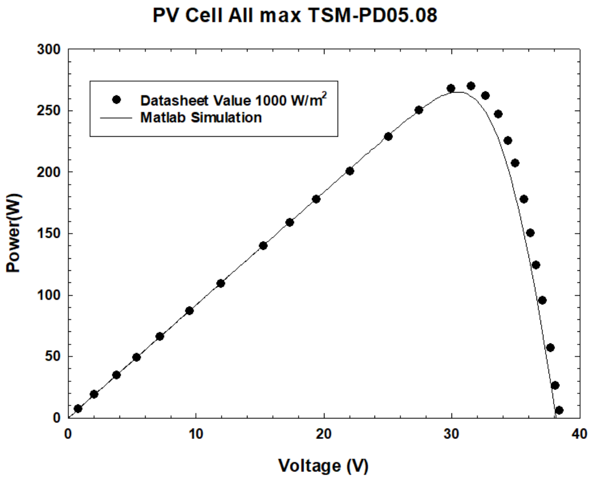

Figure 16. Comparison between the Matlab simulation and the values provided by the manufacturer of the power-voltage characteristic for an irradiation of 1000 W/m^2.

The simulations obtained with Matlab compared to the values of the curves measured by the manufacturer that we have reported give very good results.

5. Conclusion

In this paper, we have shown that starting from the one-diode model with series resistance and shunt, starting from the equation of the cell current, which is an iterative equation where the current depends on itself, and by making appropriate and physically justified approximations, we can, by a simple analytical method, obtain good values of the model parameters and obtain good simulations of the current-voltage curves I-V and power-voltage P-V.

Conflicts of Interest

The authors declare no conflicts of interest regarding the publication of this paper.

References

[1] International Energy Agency (2023) CO_2 Emissions in 2022. https://www.iea.org/reports/co2-emissions-in-2022

[2] Lun, S., Guo, T. and Du, C. (2015) A New Explicit I-V Model of a Silicon Solar Cell Based on Chebyshev Polynomials. *Solar Energy*, **119**, 179-194. https://doi.org/10.1016/j.solener.2015.07.007

[3] Dolara, A., Leva, S. and Manzolini, G. (2015) Comparison of Different Physical Models for PV Power Output Prediction. *Solar Energy*, **119**, 83-99. https://doi.org/10.1016/j.solener.2015.06.017

[4] Les cellules solaires photovoltaïques. https://www.mcours.net/cours/pdf/hassbg/hassbgli535.pdf

[5] Rodrigues, E.M.G., Melício, R., Mendes, V.M.F. and Catalão, J.P.S. (2024) Simulation of a Solar Cell Considering Single-Diode Equivalent Circuit Model. *Renewable Energy and Power Quality Journal*, **9**, 369-373. https://doi.org/10.24084/repqj09.339

[6] Liu, S.Y. and Dougal, R.A. (2002) Dynamic Multiphysics Model for Solar Array. *IEEE Transactions on Energy Conversion*, **17**, 285-294. https://doi.org/10.1109/tec.2002.1009482

[7] Sera, D., Teodorescu, R. and Rodriguez, P. (2007) PV Panel Model Based on Datasheet Values. 2007 *IEEE International Symposium on Industrial Electronics*, Vigo, 4-7 June 2007, 2392-2396. https://doi.org/10.1109/isie.2007.4374981

[8] Ould Mohamed Yahya, A., Ould Mahmoud, A.K. and Youm, I. (2008) Etude et modélisation d'un générateur photovoltaïque. *Revue des Energies Renouvelables*, **11**, 473-483. https://doi.org/10.54966/jreen.v11i3.97

[9] Yahfdhou, A., Mahmoud, A. and Youm, I. (2013) Modeling and Optimization of Photovoltaic Generator with Matlab/Simulink. *International Journal of I Tech and E Engineering*, **3**, 108-111.